processes

MDPI

Article

Experimental Study on Optimizing Steam Solvent Co-Injection Process in Akan Carbonate Oilfield

Muneer A. Suwaid [1,*], Ilgiz F. Minkhanov [1], Mikhail A. Varfolomeev [1,*], Ameen A. Al-Muntaser [1], Alexander V. Bolotov [1], Richard Djimasbe [1], Shadi A. Saeed [1], Dmitrii A. Emelianov [1], Ruslan K. Khairtdinov [2], Aidar I. Sattarov [2] and Mohammed Amine Khelkhal [1,*]

[1] Department of Petroleum Engineering, Kazan Federal University, 18 Kremlyovskaya Str., 420008 Kazan, Russia
[2] CJSC "Enterprise Kara Altyn", 48 Shevchenko Str., Almetyevsk District, Republic of Tatarstan, 423450 Almetyevsk, Russia
* Correspondence: suwaidmuneer@gmail.com (M.A.S.); vma.ksu@gmail.com (M.A.V.); amine.khelkhal@gmail.com (M.A.K.)

Abstract: Steam solvent co-injection processes are generating considerable interest in terms of improving heavy oil upgrading in unconventional reservoirs. The characteristics of the opted solvents in the field have not been dealt with in depth. This paper presents a study on selecting the most optimal solvent for the Akan oilfield enhanced oil recovery (EOR). The first step in this work consisted of determining the Akan oil field viscosity, through an elemental and SARA analyses. Next, a set of physical and chemical methods was used to understand the mechanism of solvents' effect on oil viscosity dynamics. The compositions of the used solvents were analyzed by a gas chromatography-mass spectrometer system equipped with a mass selective detector ISQ (USA). The evidence from the present study suggests that toluene and o-xylene are the most optimal solvents for enhancing the Akan oil recovery and reducing its viscosity. The obtained data demonstrated a higher efficiency of the used solvents on the oil viscosity reduction where the maximum oil viscosity reduction was observed in the presence of toluene, which led to a value of 178.1 mPa.s. Moreover, the obtained results reported that the solvent co-injection process efficiency increases gradually depending on the chemical composition of the used solvent, as witnessed by the obtained oil recovery factor (RF) values. It has been found that the oil recovery factor values during the capillary soaking in the presence of water was equal to 20%, in the presence of o-xylene it was equal to 61%, and in the presence of toluene, it was equal to 69%. Likewise, a similar efficiency behavior has been demonstrated during filtration experiments where water led to a 26% recovery factor, o-xylene to 69%, and toluene to 78%, meanwhile the solvent slug led to 65%. The results of this study would seem to suggest that the viscosity of the investigated oil decreases in the presence of aromatic solvents, such as toluene and o-xylene, as witnessed by the recovery factors they demonstrated. A consequence of these changes is the possibility that aromatic solvent molecules tend to separate the asphaltene layers and reduce the overlap between large asphaltene macromolecules, which leads to the dissociation of asphaltene aggregates.

Keywords: enhanced oil recovery; steam injection; solvent; recovery factor; capillary soaking

check for updates

Citation: Suwaid, M.A.; Minkhanov, I.F.; Varfolomeev, M.A.; Al-Muntaser, A.A.; Bolotov, A.V.; Djimasbe, R.; Saeed, S.A.; Emelianov, D.A.; Khairtdinov, R.K.; Sattarov, A.I.; et al. Experimental Study on Optimizing Steam Solvent Co-Injection Process in Akan Carbonate Oilfield. *Processes* **2023**, *11*, 459. https://doi.org/10.3390/pr11020459

Academic Editor: Qingbang Meng

Received: 8 December 2022
Revised: 20 January 2023
Accepted: 31 January 2023
Published: 3 February 2023

1. Introduction

Until now, modern society is still highly dependent on a stable source of energy in order to achieve daily production and satisfy demands. It is common knowledge that oil is the main source of energy nowadays. A recent 'Statistical Review of World Energy' provided by BP has estimated the world's proven oil reserves to 1.6 trillion barrels which are planned to be exploited within the next 50 years. However, the amount of these reserves would mainly come from unconventional sources, which are more difficult and expensive to produce [1,2].

Unconventional oil reserves are mainly composed of heavy and extra-heavy oil, which are produced by enhanced oil recovery methods (EOR). EOR is a set of methods designed to extract heavy oil based on different techniques, such as in-situ combustion, which is based on injecting air into the reservoir, and initiate the combustion of oil in place in order to increase the reservoir temperature and hence decrease the viscosity of heavy oil [3,4]. Other techniques are based on applying electromagnetic heating and the catalytic application, such as reservoir microwave heating in the presence of transition metal based catalysts which are able to improve the heating flow and consequently the oil mobility within the reservoir [5–7]. Likewise, water steam injection has been reported to be one of the widely applied techniques in the field of heavy oil enhanced recovery. It is based on injecting hot water steam into the reservoir, and as a result of the heat flow and exchange, the high molecular compounds contained in the heavy oil break down and turn into light oil components which lead to oil viscosity reduction and hence is easy to recover [8–10].

Regardless of the importance of the aforementioned EOR methods, they are still very far from real application in the field. Nevertheless, steam injection methods are still widely used methods in extracting and producing heavy oil reserves. Steam assisted gravity drainage (SAGD) [11–15] is commonly known to be the most common thermal recovery method. It is based on injecting steam into the reservoir for creating hot zones able to decrease the oil viscosity and increase its flow by gravity, and thus, its easy production from the well [16,17].

One of the main issues concerning the knowledge about the application of the SAGD process is the lack of control over the high energy and water consumption, CO_2 emissions, and the cost of the post-production water treatment [18,19]. Most studies regarding minimizing the environmental impacts and operating costs of SAGD have tended to focus on the application of several catalytic systems or developing hybrid systems, which combines it with other enhanced oil recovery techniques. One of the most practical solutions proposed for improving the SAGD technique is the solvent co-injection with water steam [8]. In fact, the injection of a solvent contributes to the additional washing of heavy oil from the rock and increases the drainage zone of wells [20–24]. Thus, the quantity of steam required is minimized to produce the same amount of oil that can be obtained by the classical SAGD.

Experts have always seen the application of solvents based on aliphatic and aromatic hydrocarbons and their mixtures during SAGD as a promising approach to improve the enhanced oil recovery during steam stimulation processes [20,23,25–27]. In their work, Naser et al. conducted the first solvent/steam injection experiment by injecting naphtha with steam. The obtained results witnessed a significant improvement in oil recovery in the presence of the used solvents, compared to the traditional SAGD process [26]. In addition, Zare, Alireza, et al. studied the effectiveness of the co-injection of aliphatic hydrocarbon solvents as an additive similar to butane, pentane, hexane, heptane, and octane with steam at low pressure to enhance the heavy oil recovery. The obtained results revealed that co-injecting these solvents with steam leads to an efficient oil recovery. In addition, it has been found that these solvents were able to reduce the cumulative steam oil ratio, especially the lighter solvents, such as hexane, which was found to be the best performing solvent in terms of oil recovery at 20 wt.% [23].

Keshararz et al. proved that the optimal solvents are those with the most identical thermo-physical characteristics to water under pressure and temperature conditions in the steam chamber [27]. In a similar study, Fatemi et al. studied the content of several solvents in order to improve the heavy oil recovery from existing reservoirs. The authors reported that they were able to determine the solvent type for the specific operating conditions in which the reservoir and fluid properties result in an ideal solvent volatility [20].

This paper sheds light on the co-injection of different solvents during the development of the Akan oilfield by steam injection enhanced oil recovery method. A solvent compatible with oil properties was selected to ensure the heavy crude oil viscosity reduction and maximum recovery, and a physical modeling on a composite model was conducted, taking into account the reservoir conditions at the Akan oilfield.

2. Materials and Methods

2.1. Materials

An oil and core sample extracted from the Akan oilfield was used in laboratory conditions to perform the steam co-injection process experiments. The studied solvents in this work were composed of toluene, benzene, o-xylene, benzyl alcohol, isopropyl alcohol, ethyl acetate, methyl tert-butyl ether (MTBE), nefras, commercial solvent (CS), and petroleum ether and their mixture.

2.2. Viscosity, Elemental, and SARA Analysis

The SVM-3000 Stabinger viscometer (Anton Paar, Graz, Austria) was used to determine the viscosity of the studied oil samples. The elemental composition analysis (carbon, hydrogen, nitrogen, oxygen, and sulfur) of the heavy oil samples before and after upgrading, was performed using a PerkinElmer 2400 Series II instrument (PerkinElmer, Waltham, MA, USA). The saturated hydrocarbons, aromatic compounds, resins, and asphaltenes (SARA) analysis of all of the studied oil samples was performed, according to the ASTM D 4124 method [28].

2.3. Gas Chromatography-Mass Spectrometry (GC-MS) Analysis

The compositions of a multicomponent commercial solvent and a mixture of individual solvents were analyzed by gas chromatography-mass spectrometry equipped with a mass selective detector ISQ (Thermo Fisher Scientific, Waltham, MA, USA). The components of the samples were identified using the NIST electronic library of mass spectra together with the literature data, as described in detail in the work of Chemodanov et al. [29].

2.4. Evaluation of the Degree of Turbidity of the Solvents and Their Compositions in Oil

The measurements were carried out on a Hach 2100AN turbidity meter (Hach Company, Ames, IA, USA). Prior to completing the measurements, the device was warmed up for at least half an hour and then calibrated against the standard solutions of Hach StabCal formazin in the range of 0.1–7500 NTUs (nephelometric turbidity units). The studied samples were placed in cylindrical cuvettes, the outer surface of which was wiped with silicone oil before the measurements were taken. The turbidity readings for each sample were recorded at least 5 times followed by obtaining the arithmetic mean.

2.5. Solvent's Thermal Analysis

The experiments on the solvent's thermal stability were performed on a TG209 F1 Libra precision thermogravimeter (Netzsch GmbH, Selb, Germany), combined with an Alpha FT-IR spectrometer (Bruker GmbH, Billerica, MA, USA) using a transit line for analyzing the gaseous products.

2.6. Porosity and Permeability Determination

A gas porosimeter-permeameter Plast-215ATM (Agrosy Technologies company, Irvine, CA, USA) was used to determine the porosity and permeability of the studied samples. Micro and nanofocus X-ray control system for computed tomography General Electric V | tome | X S 240 (Frankfurt am Main, Germany) was used to determine the void ratio of the core sample.

2.7. Filtration Experiments

Filtration studies on the solvent co-injection with steam were carried out on a laboratory unit to determine the oil displacement efficiency under thermal exposure. For the experiments with steam only and steam with solvent, the core samples were taken from the desiccator, which were wiped with filter paper for oil, weighed, and then placed in a core holder. The cores were positioned in the core holder according to the diagram shown in Figure 1 and compacted.

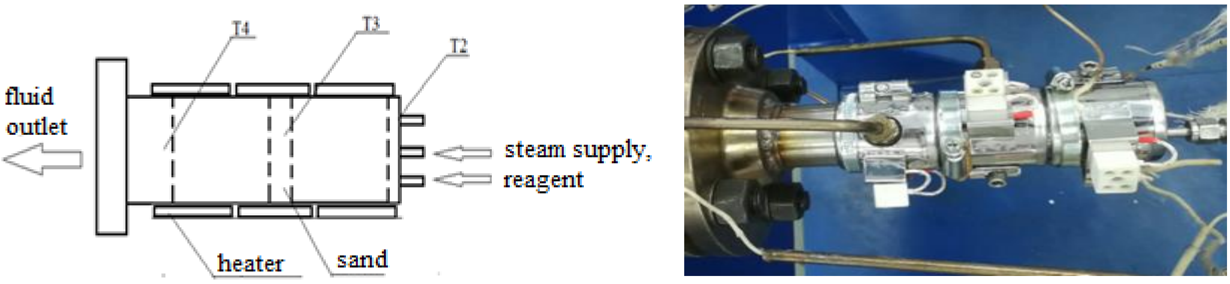

Figure 1. The layout of the thermocouples in the core holder.

3. Results and Discussion

3.1. Determination of the Group and Elemental Composition of the Heavy Oil

The group and elemental composition analysis of the studied heavy oil was conducted in order to select the appropriate solvents. The obtained data are presented in Table 1.

Table 1. Heavy oil physical properties and SARA analysis.

Group Composition, Weight%			
Saturated Hydrocarbons	Aromatic Hydrocarbons	Resins	Asphaltenes
34.97 ± 0.5	36.37 ± 0.6	18.93 ± 0.5	9.73 ± 0.3
Elemental Composition, %			
C	H	N	N_H/N_C
83.30	11.97	0.37	1.72

According to the results of the SARA analysis, it can be noted that the studied oil contains a large amount of resins (18.93 ± 0.5%) and asphaltenes (9.73 ± 0.3%), which, on the one hand, determine its high viscosity, and on the other hand, they may serve as natural emulsifiers (promote the formation of an emulsion).

3.2. Study of the Rate and Completeness of the Oil Dissolution in Selected Solvents and Their Mixtures in a Different Ratio

Various solvents were selected in this work to reduce the heavy oil viscosity, including individual and multicomponent compositions based on aliphatic and aromatic hydrocarbons, as well as other classes of organic compounds. The physical and chemical composition of the used solvents is presented in Table 2.

Table 2 shows the main characteristics of the opted solvents in this study. The process of the optimal solvents' selection has been followed by the criteria of the structure of organic solvents and the functional fragments in various ratios of their composition. Solvents with different types of functional groups and different compositions were selected to study the completeness and dissolution rate by the adiabatic calorimetry method as follows:

- Alkanes: heptane,
- Arenas: toluene, o-xylene,
- Polar oxygen-containing structures: ethyl acetate, MTBE,
- Mixtures of individual solvents: toluene/ethyl acetate/heptane (40:40:20), toluene/ethyl acetate (72:25),
- Mixtures of industrial solvents: CS, nefras, toluene/nefras (75:25).

It is common knowledge that dissolution heats (ΔH_{solv}) are composed of the intermolecular interactions energy (ΔH_{int}) and the formation energy of a "cavity" (ΔH_{cav}) which places the sorbate into the volume of the solvent, when considering the of change regularities in the dissolution heats depending on the substances whose structural features are under study. However, an increase in the energy of cavity formation was observed

($\Delta H_{cav}{}^{heptane} = 0$ kJ/mol, $\Delta H_{cav}{}^{toluene} = 2.65 \times 10^{-2}$ kJ/mol) when passing from non-polar paraffinic solvents (heptane) to aromatic (toluene, o-xylene) and oxygen-containing (MTBE, ethyl acetate) solvents.

Table 2. Physical properties and chemical composition of the used solvents.

No.	Sample	Composition, %				
		Non-Polar Solvent				Polar Solvent
		Aromatics	Naphthenes	Alkanes	Isomers of Alkanes, etc.	
1.	Heptane	-	-	100	-	-
2.	Dodecane	-	-	100	-	-
3.	Toluene	100	-	-	-	-
4.	Benzene	100	-	-	-	-
5.	O-xylene	100	-	-	-	-
6.	Benzyl alcohol	100	-	-	-	+
7.	Isopropyl alcohol	-	-	-	-	100
8.	Ethyl Acetate	-	-	-	-	100
9.	Methyl tert-butyl ether (MTBE)	-	-	-	-	100
10.	Nefras	20.53	15.77	17.06	46.64	-
11.	Commercial solvent (CS)	23.45	1.48	23.68	51.39	-
12.	Petroleum ether	-		100		-
13.	Toluene/Heptane (50:50)	50	-	50	-	-
14.	Toluene/Petroleum ether (50:50)	50		50		-
15.	Heptane/Ethyl Acetate: (50:50)	-	-	50	-	50
16.	Toluene:MTBE: (75:25)	75	-	-	-	25
17.	Toluene:Ethyl Acetate (50:50)	50	-	-	-	50
18.	Toluene:Ethyl Acetate:Heptane (40:40:20)	40	-	20	-	40
19.	Toluene:Ethyl Acetate (75:25)	75	-	-	-	25
20.	Toluene:Ethyl Acetate (25:75)	25	-	-	-	75
21.	Ethyl cellosolve	-	-	-	-	100
22.	CS-1	52.96		47.04		
23.	CS-2	67.66		32.34		
24.	Toluene/CS (50:50)	61.73		38.27		
25.	Toluene/Nefras (50:50)	60.27		39.73		

The results of the calorimetric measurements (Table 3), showed only the endo-effect of dissolution in the studied solvents. This means that there was no energy absorption during the dissolution of the oil components and their further interaction with any of the solvents. Moreover, the absence of the thermal effect ($\Delta H_{solv} = 0$) has been observed in isopropanol, where there was a separation of the solvent oil phases and the absence of intermolecular interaction; therefore, this solvent was not recommended for further applications. Furthermore, the thermal effect of dissolution was found to be equal to zero ($\Delta H_{solv} = 0$) in heptane, while the formation enthalpy of the cavity was also found to be equal to zero ($\Delta H_{cav}{}^{heptane} = 0$). This led us to conclude that there is no gain in energy in the formation of intermolecular bonds between oil components and heptane. However, further rheological studies are recommended to exclude heptane and aliphatic solvents. Moreover, the maximum values of the dissolution endo-effect were observed for ethyl acetate, MTBE, toluene/ethyl acetate mixture (−14.5; −14.1; −14.2 J/g), which is associated with a high-energy consumption for the rupture and cavity formation in the polar solvents, such as ethyl acetate and MTBE. At the same time, the rate of formation of the new bonds upon dissolution in MTBE was found to be two times higher than that in ethyl acetate and in the ethyl acetate/toluene mixture. It is worthy to note that despite the deep dissolution degree found in energy-intensive polar solvents, such as MTBE and ethyl acetate, further studies on changing the viscosity and achieving aggregation stability are importantly required. It can be noted that the ΔH_{cav} values of toluene and o-xylene, are representatives of aromatic hydrocarbons, homologues and differ by one methylene group, and differ by a factor of 2. In this case, the enthalpies and dissolution time in toluene (10.9 J/g, 90 s) were found to be much longer than in o-xylene (2.3 kJ/mol, 60 s) which indicates a deeper dissolution in toluene. In fact, aromatic solvents were recommended for further research. For mixed solvents, intermediate values of the enthalpy of dissolution were found, and they were also included in further studies.

Table 3. Oil dissolution heat and time in various pure solvents and their mixtures.

Solvent	ΔH, J/g	T, s
Commercial solvent (CS)	2.9	60
Nefras	8.7	50
Ethyl Acetate	14.5	80
Heptane	0	0
Methyl tert-butyl ether (MTBE)	14.1	40
Toluene	10.9	90
Isopropanol	0	0
O-xylene	2.3	60
Toluene:ethyl acetate (75:25)	3.6	40
Toluene:ethyl acetate (75:25)	14.2	100

It is suggested that forming “suitable” solvation shells around the particle-aggregates of asphaltenes is important for the rupture of aggregates and the formation of a stable solution for the possible dissolution of oil in solvents [30–32].

3.3. Oil Viscosity Study in the Presence of Several Solvents and Their Mixtures at Different Concentrations

Figure 2 shows the results of the initial oil viscosity at different temperatures. The viscosity of the initial oil was found to be equal to 427.18 mPa.s at 25 °C.

The research team prepared various solutions consisting of oil and solvents with concentrations of 1, 2 and 3% by mass, in order to investigate the effect on the oil viscosity. Viscosity measurements were taken at 25 °C, and the results are displayed in Table 4.

The effectiveness of the solvents used (3% wt.) was evaluated based on their ability to decrease the oil viscosity using the following criterion: less than 40%—low efficiency, not recommended for use; 40–50%—effective, application is possible, continued research; more than 50%—high efficiency, further research is needed. According to the obtained criteria, benzyl alcohol was excluded from further research (38%). Moreover, benzene, showed a 41% efficiency, but as it is a substance of the second hazard class, it was also excluded from further studies. High efficiency in viscosity reduction was observed for heptane, toluene, o-xylene, ethyl acetate, petroleum ether, toluene/ethyl acetate mixtures (50:50) and ethyl cellosolve. Nevertheless, the decrease in viscosity in aliphatic and polar solvents can also be explained by the precipitation of the asphaltene particles due to the destabilization of colloids. In aromatic compounds, the viscosity decrease was the result of their dissolution. Therefore, for all solvents, except for benzene and benzyl alcohol, studies were carried out to determine their aggregation stability.

Table 4. Changes in the oil viscosity dynamics in the presence of different solvents.

No.	**Sample**	**Solvent Concentration, % wt.**		
		1	**2**	**3**
		Viscosity at 25 °C, mPa.s		
1.	Heptane	313.3	290.8	183.4
2.	Dodecane	321.1	276.8	245.2
3.	Toluene	301.8	266.3	178.1
4.	Benzene	324.5	289.1	252.6
5.	O-xylene	298.2	256.1	208.4
6.	Benzyl alcohol	378.8	354.8	264.5
7.	Isopropyl alcohol	342.8	268.2	226.8
8.	Ethyl acetate	315.7	252.9	198.8
9.	Methyl tert-butyl ether (MTBE)	308.9	261.1	225.1
10.	Nefras	336.9	316.4	233.1
11.	Commercial solvent (CS)	301.1	274.0	244.8
12.	Petroleum ether	319.9	279.8	190.8
13.	Toluene/nephras (50:50)	291.2	277.5	248.3
14.	Toluene/petroleum ether (50:50)	279.7	270.5	243.9
15.	Heptane/ethyl acetate: (50:50)	282.4	278.9	249.5
16.	Toluene/MTBE (75:25)	312.4	262.7	253.7
17.	Toluene:ethyl acetate (50:50)	279.1	219.1	200.5
18.	Toluene:ethyl acetate (75:25)	350.8	280.4	218.5
19.	Toluene:ethyl acetate (25:75)	372.4	322.9	227.8
20.	Ethyl cellosolve	312.9	280.1	213.5
21.	CS-1	317.7	273.4	258.9
22.	CS-2	326.5	277.8	234.4
23.	Toluene/CS (50:50)	300.6	259.0	233.3
24.	Toluene/nephras (50:50)	337.9	292.9	253.8

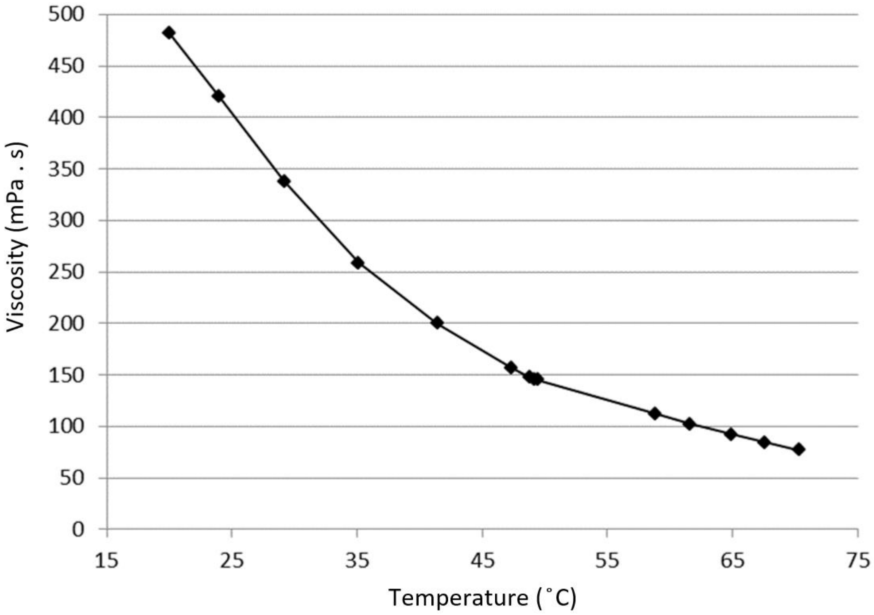

Figure 2. Initial oil viscosity depending on temperature.

3.4. Oil Solutions Aggregation Stability in Several Solvents and Their Mixtures at Different Ratios

The obtained results from turbidity measurements are presented in Table 5. Two areas were distinguished for all of the investigated solutions: oil solutions (3% wt.) with NTU $\leq$ 1.1 and oil solutions (3% wt.) with NTU $\geq$ 91. The following criteria were established to assess the oil/solvent stability: (1) NTU $\leq$ 1—effective solvents recommended for use; (2) NTU $\geq$ 50—ineffective solvents not recommended for further tests.

Table 5. Experimental values of the oil solution turbidity in various solvents and their mixtures.

No.	Measurement Number	Solvent	Oil, Mass. %	Nephelometric Turbidity Unit, NTU
1.	1.	Heptane	1	490
	2.		2	1091
	3.		3	1665
2.	4.	Dodecane	1	140
	5.		2	269
	6.		3	439
3.	7.	Toluene	1	0.60
	8.		2	0.26
	9.		3	0.21
4.	10.	Ethyl Acetate	1	554
	11.		2	3280
	12.		3	4186
5.	13.	Commercial solvent (CS)	1	165
	14.		2	334
	15.		3	636
6.	16.	Nefras	1	152
	17.		2	389
	18.		3	532

Table 5. *Cont.*

No.	Measurement Number	Solvent	Oil, Mass. %	Nephelometric Turbidity Unit, NTU
7.	19.	Petroleum ether	1	478
	20.		2	464
	21.		3	1245
8.	22.	Toluene/heptane 50:50	1	1.10
	23.		2	0.81
	24.		3	0.31
9.	25.	Toluene/petroleum ether 50:50	1	0.66
	26.		2	0.43
	27.		3	0.35
10.	28.	Heptane/ethyl acetate: (50:50)	1	162
	29.		2	380
	30.		3	610
11.	31.	Methyl tret butyl ether (MTBE)	1	278
	32.		2	291
	33.		3	649
12.	34.	Toluene/MTBE (75:25)	1	0.63
	35.		2	0.30
	36.		3	0.27
13.	37.	Toluene:ethyl acetate (50:50)	1	91.2
	38.		2	123
	39.		3	157
14.	40.	Toluene:ethyl acetate (75:25)	1	0.58
	41.		2	0.31
	42.		3	0.22
15.	43.	Toluene:ethyl acetate (25:75)	1	286
	44.		2	852
	45.		3	1534
16.	46.	Ethyl cellosolve	1	did not dissolve
	47.		2	
	48.		3	
17.	49.	CS-1	1	0.74
	50.		2	0.49
	51.		3	0.39
18.	52.	CS-2	1	0.90
	53.		2	0.61
	54.		3	0.49
19.	55.	Toluene/CS (50:50)	1	0.97
	56.		2	0.63
	57.		3	0.48

Table 5. *Cont.*

No.	Measurement Number	Solvent	Oil, Mass. %	Nephelometric Turbidity Unit, NTU
20.	58.	Toluene/nephras (50:50)	1	0.57
	59.		2	0.32
	60.		3	0.24
21.	61.	O-xylene (50:50)	1	0.51
	62.		2	0.28
	63.		3	0.22
22.	64.	Toluene/ethyl acetate/heptane (40:40:20)	1	0.83
	65.		2	0.42
	66.		3	0.32

According to the obtained results, heptane, dodecane, ethyl acetate, and MTBE did not fall within the list of the recommended solvents included. In addition, it has been found that oil does not dissolve in ethyl cellosolve, which also excludes it from further research. Moreover, heptane/ethyl acetate (50:50), toluene/ethyl acetate (50:50), toluene/ethyl acetate (25:75) were found to not be recommended mixtures of individual solvents. It should be noted that the toluene/ethyl acetate mixture (75:25) shows generally good results (NTU < 1), from which it can be concluded that the stabilization of the asphaltene particles is due to the addition of toluene to the mixture. Moreover, the absence of colloidal particles was achieved at a toluene to ethyl acetate ratio of 75:25. It can also be concluded that mixed compositions from individual solvents and industrial mixtures—toluene/heptane (50:50), toluene/petroleum ether (50:50), toluene/MTBE (75:25), toluene/ethyl acetate/heptane (40:40:20), toluene/ethyl acetate (75:25), toluene/CS (50:50), toluene/Nefras (50:50) and toluene/ethyl acetate/heptane (40:40:20) have low NTU values, only due to the presence of toluene in the mixture. Such mixtures cannot be recommended due to the possible change in composition during filtration and clogging of the core material with colloidal particles of asphaltenes. The obtained results led us to propose toluene, o-xylene, CS-1 and CS-2 as recommended solvents and compositions, as shown by their turbidity values.

Following the study of the impact of various solvents and their compositions on the properties of Akan oil, such as viscosity, turbidity and calorimetry, the research team selected toluene and o-xylene for further investigation.

3.5. Solvent's Thermal Analysis

The thermal stability of toluene and o-xylene was determined by means of thermogravimetric analysis. The obtained thermal properties of the studied solvents are presented in Table 6.

Table 6. Solvent's thermal stability parameters.

Solvent	Temperature of the Maximum Intensity of the Process, °C	End of Process Temperature, °C
Toluene	76.2	81.0
O-xylene	105.6	110.4

The obtained results (Table 6) showed that o-xylene has the highest thermal stability, which correlates with its highest boiling point T = 144 °C among the studied samples. In addition, the thermogravimetric curves (Figure 3) show that all solvents occur completely evaporated already at 110.4 °C (in the case of o-xylene). This is explained by its high volatility at atmospheric pressure. It is common knowledge that DTG curves are the derivatives of the weight loss curves shown in Figure 3 (dotted lines). The obtained curves demonstrate a one-stage behavior for all of the studied processes. This stage corresponds to the transition of solvents from the liquid phase to the vapor phase (evaporation). During the analysis of the IR spectra of gaseous products, it was confirmed that they are represented by the original solvent molecules.

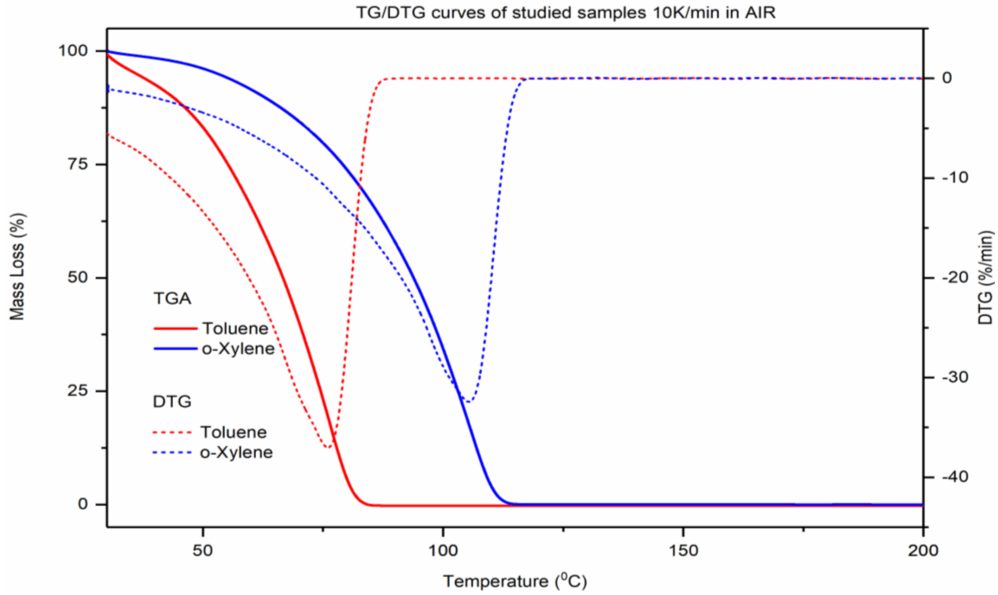

Figure 3. TG-DTG curves of the analyzed solvents (o-xylene (blue), toluene (red)).

According to the thermal stability criteria, all of the selected solvents (toluene, xylene) are suitable for the next stage of steam filtration and enhanced oil recovery.

3.6. Core Preparation

In order to study the effect of the solvents on oil recovery, three core samples (1c, 4c and 8c) were taken from well 2441 of the Akan field. Further, from the selected samples, standard cylindrical samples were drilled, with a diameter of 30 mm and a length of 50 mm. Following the preparation of the standard samples, the extraction stage began. Extraction of the samples was carried out by standard hot extraction with a mixture of solvents (chloroform + carbon tetrachloride + alcohol + benzene) according to the Russian standard (GOST R 55878-2013, GOST 9572-93) in a Soxhlet apparatus. The degree of extraction was checked out with an ultraviolet lamp, and the hydrocarbons were completely removed from the samples. Following the extraction, standard studies were carried out on the samples to determine the porosity and permeability. Table 7 shows the porosity, permeability, and void ratio of the extracted samples. According to the obtained results, the core 8c has the maximum permeability and porosity, as shown in the Table 7.

Table 7. Porosity, permeability, and void ratio of the extracted samples.

No.	Weight before Extraction, g	Weight after Extraction, g	Porosity, %	Permeability, mD	Void Ratio, %
1c	74.445	72.114	16.52	64.18	2.60
4c	80.043	78.203	12.2	58.75	1.34
8c	77.343	74.066	18.87	65.08	2.14

Computed tomography was utilized to calculate the void ratio values (Table 7). Figure S1 (Supplementary Material) shows the orthogonal X-ray density sections of the studied samples and three-dimensional visualization of the shape of the void space of the studied samples.

3.7. Study of the Capillary Soaking of an Oil-Saturated Model

For the soaking experiments, test core samples (1c, 4c and 8c) were placed in a glass container filled with formation water or solvent (formation water (1), toluene (2) and o-xylene (3)), respectively. The samples were hermetically sealed and left for 7 days. Table 8 presents the main obtained parameters and results.

Table 8. The main parameters for conducting soaking experiments.

Experiment	Core Sample, 30 × 50 mm	Core Weight before Impregnation, g	Solvent Weight, g	The Volume of Oil in the Initial Core$_{\mathrm{Vinit.}}$, mL	Displaced Oil Volume V_d, mL *	RF, %
1	1c	76.3456	75	3.47	0.70	20
2	4c	82.2514	75	2.87	1.98	69
3	8c	80.2091	75	4.09	2.50	61

* Determined by UV-VIS spectrophotometry.

The recovery factor (RF) by water and solvents during soaking was calculated by the formula: RF = V_d/V_{init}.

According to the data obtained in Table 8, a low value of RF can be noted during the capillary impregnation with water due to the difference in the types of intermolecular bonds of fluids (hydrophobic oil + hydrophilic solvent—water), which determine the immiscible regime of oil-saturated rock soaking. By using the organic solvents in the two to three experiments, an increase in RF was observed, which is associated with a good dissolving ability of aromatic solvents. The driving energy behind soaking and solvation is the stabilization of asphaltenes and the concomitant reduction in oil viscosity. The obtained data showed good soaking values for toluene (RF = 69%). Tables S1 and S2 (Supplementary Material) show photos of the core samples before and after capillary soaking.

3.8. Filtration Studies on the Solvent Injection in the Reservoir Conditions

During the experiments, the recovery factor was determined by formation water and toluene and o-xylene solvents. Water injection was carried out at a selected rate of 3 mL/min continuously for 8 pore volumes, then 2 more pore volumes at a flow rate of 10 mL/min. The conditions for conducting the experiments by formation water and toluene and o-xylene solvents are shown in Table 9, and the results of the experiment are shown in Table 10 and Figure 4.

Table 9. Conditions for conducting the experiments.

Type of Influence	Core Sample	Permeability, mD	Reservoir Pressure, MPa	Flow Rate, mL/min	Inlet Temperature, °C
formation water	2c 6c	460.8 480.95	10	3/8 P.V. 10/2 P.V.	23
toluene	9c 11c	154.06 153.38	10	3/8 P.V. 10/2 P.V.	23
o-xylene	12c 15c	117.97 114.54	10	3/8 P.V. 10/2 P.V.	23

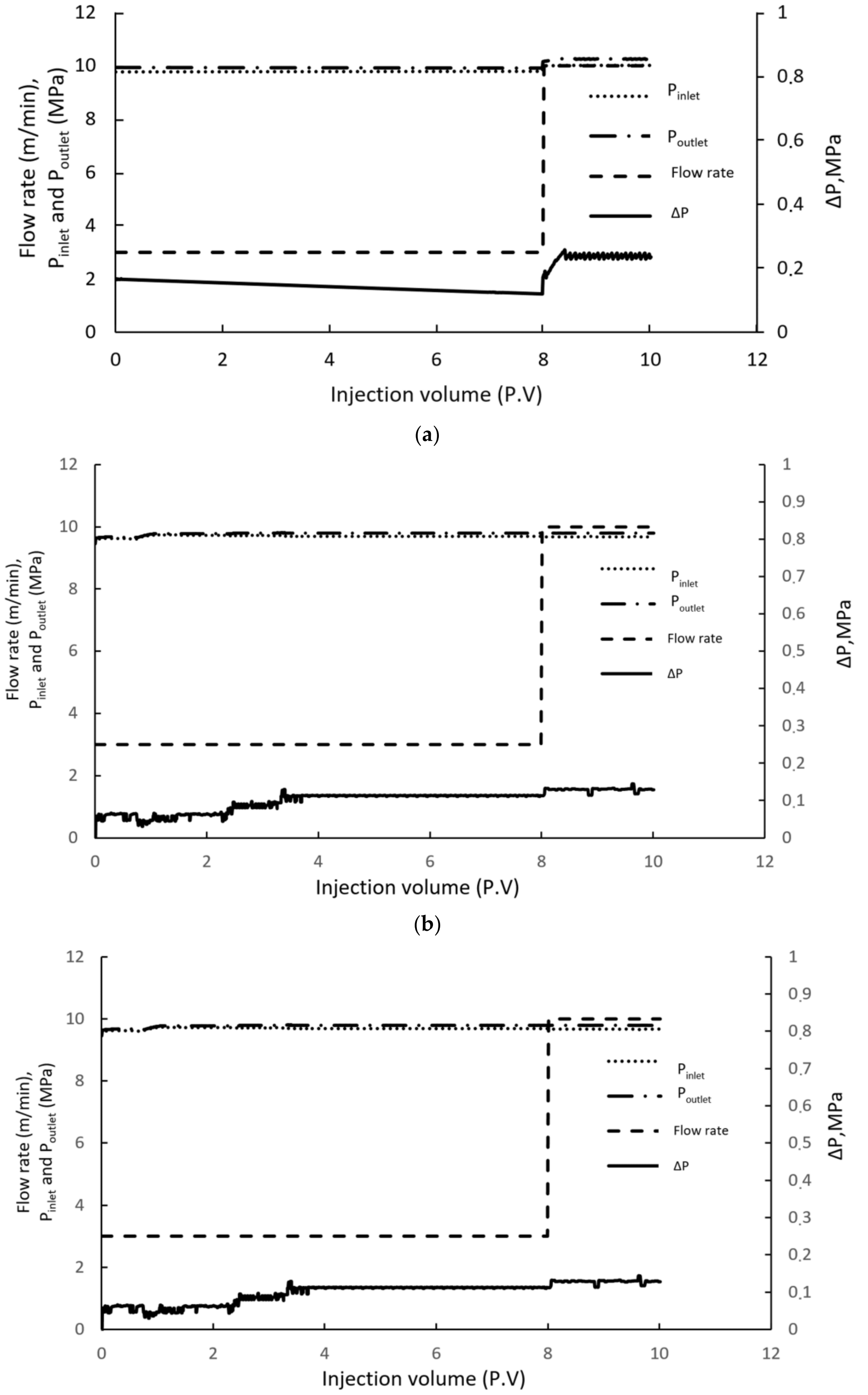

(**a**)

(**b**)

(**c**)

Figure 4. Filtration dynamics in the experiment with formation water (**a**), toluene (**b**) and o-xylene (**c**).

Table 10. Material balance in the filtration experiments.

Type of Influence	Core Sample	Oil Saturation of the Initial Core, %	Volume of Oil in the Initial Core, mL	Material Balance after the Experiment	
				Volume of Extracted Oil, mL	RF, %
formation water	2c	66	4.06	2.23	26
	6c	65	4.52		
toluene	9c	75	5.60	7.04	78
	11c	73	3.43		
o-xylene	12c	64	2.50	2.94	69
	15c	41	1.76		

A relatively low-pressure drop was observed during filtration with formation water, up to a value of 0.24 MPa, as shown in Figure 4a. Despite the lower permeability values in the experiment with toluene (153, 154 mD), compared with the experiment with water (460, 480 mD) (Table 9), an even lower pressure drop in the model was observed during filtration (up to a maximum value of 0.14 MPa), as shown in Figure 4b. These results indicate a good dissolving power of the solvent with a recovery factor of 78%. During filtration with o-xylene, a high pressure drop to 0.98 MPa was initially observed (Figure 4c), which can be explained by the heterogeneity of core 12c and 15c (Figure 5). At the same time, the recovery factor during filtration with o-xylene was 69%, as shown in Table 10.

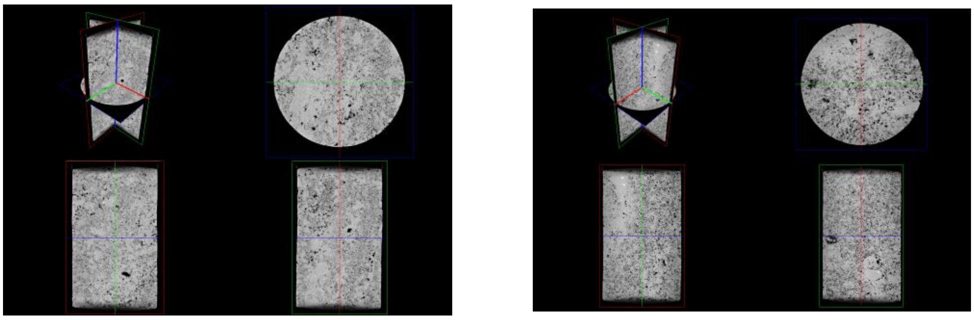

Core sample 12C Core sample 15C

Figure 5. Three-dimensional visualization of the void space shape.

3.9. Filtration Studies during the Steam and Solvent Injection on the Prepared Core Samples

During the experiments, the recovery factor by steam in the presence and absence of solvent was determined in different feed modes. Steam injection was carried out at a selected rate of 3 mL/min (by water) continuously for 8 pore volumes, then 2 more pore volumes at a flow rate of 10 mL/min. During the filtration, a pressure drop to the 0.31 bar was observed. The conditions associated to conducting the steam experiments in the presence and absence of solvent are shown in Table 11. The recovery factor was calculated, according to the formula: RF = $V_{extr.}/V_{init.}$

Where $V_{extr.}$ is the volume of oil displaced from the model, mL; $V_{init.}$—initial volume of oil in the model, mL.

Figure 6 shows the temperature profiles in the control experiment (steam). The recovery factor by steam on a composite model of an oil-saturated core from the Akan field was determined. Following filtration with steam, the recovery factor achieved was 54.7%, as shown in Table 12. During the filtration process, a pressure drop of 0.31 MPa was observed, as shown in Figure S2 (Supplementary Material).

Table 11. Conditions for conducting experiments with steam only and steam with solvent.

No.	Type of Influence	Core	Permeability, mD	Reservoir Pressure, MPa	Steam Consumption in Water, mL/min	Inlet Temperature, °C
1	Steam	3c 7c	322.5 234.13	10	3	320
2	Solvent (slug) + Steam	17c 18c	75.6 38.7	10	3	23 320
3	Steam + Solvent (mixed)	9c 11c	154.06 153.38	10	3	320

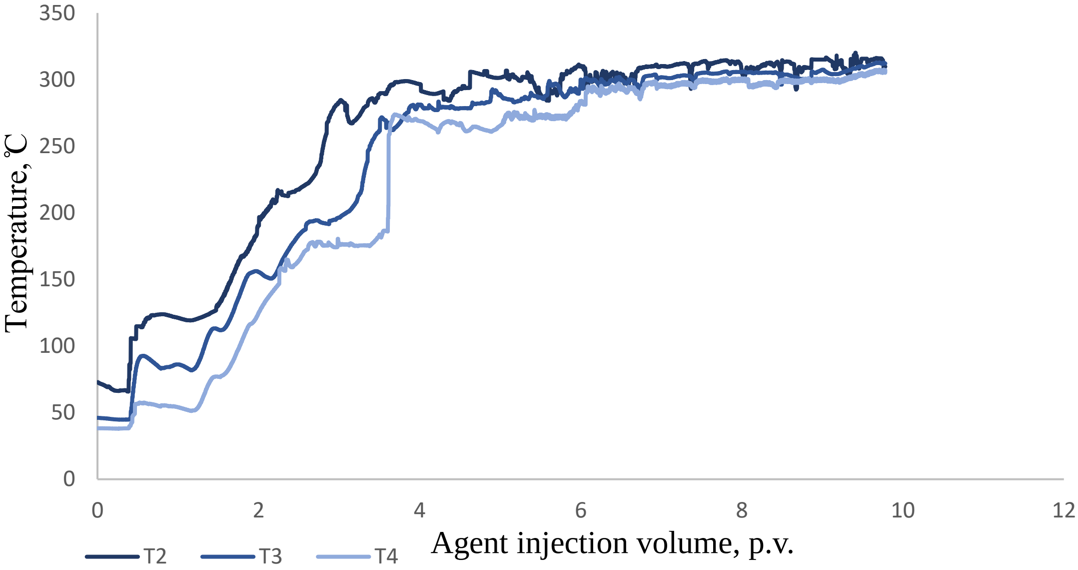

Figure 6. Temperature profiles in the control experiment.

Table 12. Material balance before and after exposure in all experiments.

Type of Influence	Core	Oil Saturation of the Original Core, %	The Volume of Oil in the Original Core $V_{init\cdot}$, mL	Material Balance after the Experiment	
				Volume of Extracted Oil V_{extr}, mL	RF, %
Steam	3c	67	3.93	4.23	54.7
	7c	65	3.81		
Solvent (slug) + Steam	17c	65	2.71	4.1	65
	18c	66	3.59		
Steam + Solvent (mixed)	9c	65	4.8	4.82	61
	11c	66	3.1		

Figure 7 shows the temperature profiles where steam with a solvent were supplied in a slug. The solvent injection was carried out at a selected rate of 3 mL/min continuously for 1 pore volume, then another 9 pore volumes of steam at a flow rate of 3 mL/min. During filtration, a pressure drop to 0.07 MPa was observed, as shown in Figure S3 (Supplementary Material). Following filtration, the recovery factor was fixed to 65%, as shown in Table 12.

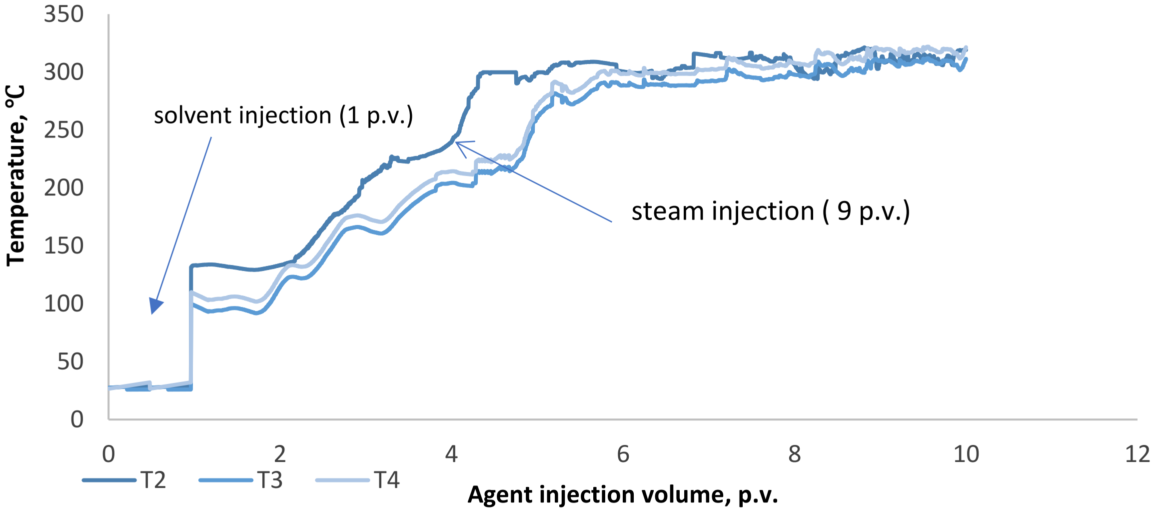

Figure 7. Temperature profiles in the experiment with steam and solvent supplied in a slug.

Figure 8 shows the temperature profiles where steam, in the presence of solvent was supplied in a mixed mode. The injection of the solvent with steam was carried out at a selected rate of 3 mL/min continuously for 10 pore volumes. During filtration, a pressure drop to 0.043 MPa was observed, as shown in Figure S4 (Supplementary Material). Following filtration, the recovery factor was 61%, as shown in Table 12.

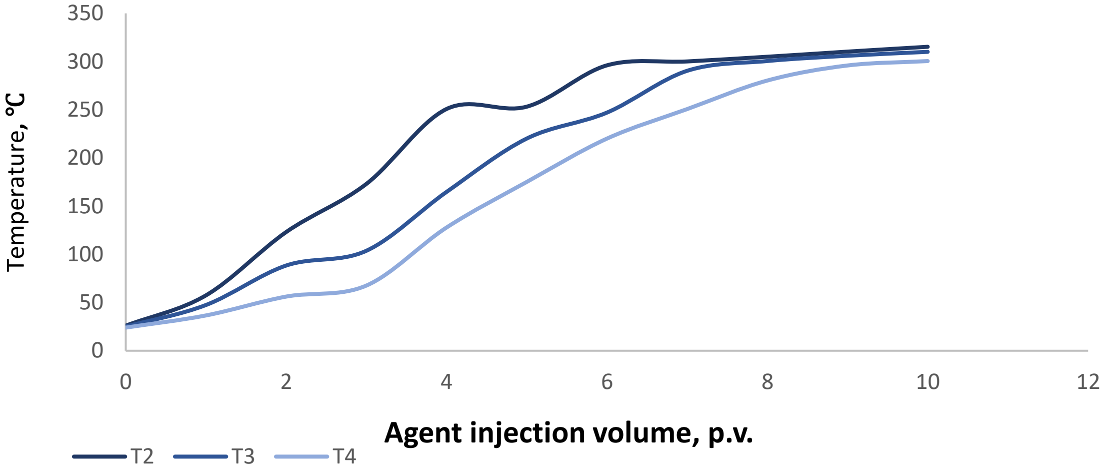

Figure 8. Temperature profiles in the experiment with steam and solvent supplied in a mixed mode.

The obtained results provide evidence for the maximum value of the recovery factor (65%) which was obtained with the solvent (slug) + steam, even though the core permeability is lower than in other experiments, as shown in the Table 12.

4. Conclusions

To sum up, the present work led us to study the characteristics of the Akan oilfield. The obtained results suggest that Akan oil contains a high amount of resins (≈19%) and asphaltenes (≈10%). Therefore, compositions based on aromatic compounds should be considered preferable from the point of view of the stabilization of colloidal asphaltene particles. Further studies were carried out to determine the viscosity of Akan oil and the aggregation stability in the presence of a series of solvents and compositions with different molecular structures and content of polar groups. The best results were found for oil solutions with toluene and o-xylene. The decrease in viscosity in aliphatic solvents (heptane, nefras, petroleum ether) is associated with the precipitation of asphaltene fraction from the solution. The obtained data found that polar solvents (ethyl acetate, MTBE) are characterized by high turbidity values. Additionally, the use of such solvents was found unsuitable due to possible clogging during injection into the reservoir. Regarding isopropanol and ethyl cellosolve, the obtained results showed phase separation, where calorimetric data indicate a high rate of oil dissolution in their presence. Moreover, most solvents exhibited the dissolution endo-effect, since the total gain in the dissolution energy was resulted from the entropy asphaltene aggregate solvation process. Capillary soaking data indicated a gradual increase in the efficiency of the studied solvents as follows: water (RF = 20%), o-xylene (RF = 61%), toluene (RF = 69%), with water as being the least effective soaking agent. Likewise, filtration experiments showed the same growth tendency in the efficiency of the studied experiments, as follows: water (RF = 26%), o-xylene (RF = 69%), toluene (RF = 78%). During the injection steam with solvent in a slug, the recovery factor was fixed at 65%.

To sum up, the results of this study suggest an opposite relation between the viscosity of the oil and the recovery factor in the presence of aromatic solvents, such as toluene and o-xylene. All of these changes can be explained by the fact that aromatic solvent molecules tend to be located between the asphaltene layers and reduce the overlap between large asphaltene macromolecules, which leads to the dissociation of asphaltene aggregates.

Supplementary Materials: The following supporting information can be downloaded at: https://www.mdpi.com/article/10.3390/pr11020459/s1. Figure S1: Orthogonal X-ray density sections and three-dimensional visualization of the shape of the void space of the samples; Figure S2: Pressure profiles at the inlet, outlet of the model, pressure drop and water flow in the control experiment (steam); Figure S3: Pressure profiles at the inlet and outlet of the model, pressure drop and water flow in the experiment (steam with a solvent was supplied in slug); Figure S4: Pressure profiles at the inlet and outlet of the model, pressure drop and water flow in the experiment (steam with the solvent was supplied in a mixed mode); Table S1: Appearance of the solution (solvent + oil) before and after soaking; Table S2: The oil-saturated core model before and after soaking.

Author Contributions: M.A.S.: Conceptualization, Methodology, Writing–Reviewing and Editing, Visualization, Supervision, Formal analysis, Investigation. I.F.M.: Investigation, Formal analysis, Writing–Original Draft. M.A.V.: Conceptualization, Reviewing and Editing, Supervision, Project administration, Funding acquisition. A.A.A.-M.: Conceptualization, Methodology, Writing–Reviewing and Editing, Supervision. A.V.B.: Investigation, Formal analysis. R.D.: Investigation, Formal analysis. S.A.S.: Investigation, Formal analysis. D.A.E.: Investigation, Formal analysis. R.K.K.: Investigation, Project administration, Funding acquisition, A.I.S.: Investigation, Project administration, Funding acquisition. M.A.K.: Formal analysis, Investigation, Editing–Reviewing, Visualization. All authors discussed and approved the final version. All authors have read and agreed to the published version of the manuscript.

Funding: This research received no external funding.

Data Availability Statement: Not available.

Acknowledgments: This research was funded by the subsidy allocated to Kazan Federal University for the state assignment in the sphere of scientific activities (Project No. 0671-2020-0048 of State Assignment No. 075-00216-20-05 of 04.06.2020 (Part II Section I)).

Conflicts of Interest: The authors declare no conflict of interest.

References

1. Petroluem, B. *BP Statistical Review of World Energy*; BP Plc: London, UK, 2018.
2. Simão, A.; Domínguez-Álvarez, E.; Yuan, C.; Suwaid, M.A.; Varfolomeev, M.A.; Ancheyta, J.; Al-mishaal, O.F.; Kudryashov, S.I.; Afanasiev, I.S.; Antonenko, D.A. On the Use of Metallic Nanoparticulated Catalysts for In-Situ Oil Upgrading. *Fuel* **2022**, *313*, 122677. [CrossRef]
3. Ushakova, A.S.; Zatsepin, V.; Khelkhal, M.A.; Sitnov, S.A.; Vakhin, A.V. In Situ Combustion of Heavy, Medium, and Light Crude Oils: Low-Temperature Oxidation in Terms of a Chain Reaction Approach. *Energy Fuels* **2022**, *36*, 7710–7721. [CrossRef]
4. Khelkhal, M.A.M.A.; Eskin, A.A.A.; Vakhin, A.V.A.V. Kinetic Study on Heavy Oil Oxidation by Copper Tallates. *Energy Fuels* **2019**, *33*, 12690–12695. [CrossRef]

5. Murzakhanov, F.; Ponomarev, A.; Khelkhal, M.A.; Amziane, O.; Vakhin, A.V.; Gafurov, M. Conventional and High-Field Pulsed EPR Experimental Studies on Bazhenov Oil Formation under the Influence of 50 Hz Electromagnetic Field. *Fuel* **2023**, *334*, 126580. [CrossRef]
6. Vakhin, A.V.; Khelkhal, M.A.; Tajik, A.; Ignashev, N.E.; Krapivnitskaya, T.O.; Peskov, N.Y.; Glyavin, M.Y.; Bulanova, S.A.; Slavkina, O.V.; Schekoldin, K.A. Microwave Radiation Impact on Heavy Oil Upgrading from Carbonate Deposits in the Presence of Nano-Sized Magnetite. *Processes* **2021**, *9*, 2021. [CrossRef]
7. Vakhin, A.V.; Khelkhal, M.A.; Mukhamatdinov, I.I.; Mukhamatdinova, R.E.; Tajik, A.; Slavkina, O.V.; Malaniy, S.Y.; Gafurov, M.R.; Nasybullin, A.R.; Morozov, O.G. Changes in Heavy Oil Saturates and Aromatics in the Presence of Microwave Radiation and Iron-Based Nanoparticles. *Catalysts* **2022**, *12*, 514. [CrossRef]
8. Sitnov, S.A.; Khelkhal, M.A.; Mukhamatdinov, I.I.; Feoktistov, D.A.; Vakhin, A.V. Iron Oxide Nanoparticles Impact on Improving Reservoir Rock Minerals Catalytic Effect on Heavy Oil Aquathermolysis. *Fuel* **2022**, *327*, 124956. [CrossRef]
9. Khelkhal, M.A.; Lapuk, S.E.; Buzyurov, A.V.; Ignashev, N.E.; Shmeleva, E.I.; Mukhamatdinov, I.I.; Vakhin, A.V. Thermal Behavior of Heavy Oil Catalytic Pyrolysis and Aquathermolysis. *Catalysts* **2022**, *12*, 449. [CrossRef]
10. Bagci, A.S. Steam Injection in Oil Reservoirs with Bottom Water Zone. *Energy Sources* **2005**, *27*, 1439–1447. [CrossRef]
11. Butler, R.M. Thermal Recovery of Oil and Bitumen. OSTI: Oak Ridge, TN, USA, 1991.
12. Mathews, T.A.; Cortes, J.A.; Bryant, R.; Hascakir, B. Miscible Flooding for Bitumen Recovery with a Novel Solvent. In Proceedings of the SPE Annual Technical Conference and Exhibition, OnePetro, Dubai, United Arab Emirates, 21–23 September 2021.
13. Huang, S.; Chen, X.; Liu, H.; Jiang, J.; Cao, M.; Xia, Y. Experimental and Numerical Study of Solvent Optimization during Horizontal-Well Solvent-Enhanced Steam Flooding in Thin Heavy-Oil Reservoirs. *Fuel* **2018**, *228*, 379–389. [CrossRef]
14. Edmunds, N.R.; Kovalsky, J.A.; Gittins, S.D.; Pennacchioli, E.D. Review of Phase A Steam-Assisted Gravity-Drainage Test. *SPE Reserv. Eng.* **1994**, *9*, 119–124. [CrossRef]
15. de Haas, T.W.; Fadaei, H.; Guerrero, U.; Sinton, D. Steam-on-a-Chip for Oil Recovery: The Role of Alkaline Additives in Steam Assisted Gravity Drainage. *Lab Chip* **2013**, *13*, 3832–3839. [CrossRef] [PubMed]
16. Chung, T.; Bae, W.; Lee, J.; Lee, W.; Jung, B. A Review of Practical Experience and Management of the SAGD Process for Oil Sands Development. *Energy Sources Part A Recovery Util. Environ. Eff.* **2011**, *34*, 219–226. [CrossRef]
17. Speight, J.G. *Enhanced Recovery Methods for Heavy Oil and Tar Sands*; Elsevier: Amsterdam, The Netherlands, 2013; ISBN 0127999884.
18. Mohammadzadeh, O.; Rezaei, N.; Chatzis, I. Production Characteristics of the Steam-Assisted Gravity Drainage (SAGD) and Solvent-Aided SAGD (SA-SAGD) Processes Using a 2-D Macroscale Physical Model. *Energy Fuels* **2012**, *26*, 4346–4365. [CrossRef]
19. Suranto, A.M.; Bae, W.; Permadi, A.K. An Investigation of Hybrid Steam-Solvent Injection for Increasing Economy and Reducing CO_2 Emission. *Pet. Sci. Technol.* **2015**, *33*, 302–310. [CrossRef]
20. Fatemi, S.M. The Applicability of Expanding Solvent Steam-Assisted Gravity Drainage (ES-SAGD) in Fractured Systems. *Pet. Sci. Technol.* **2010**, *28*, 1906–1918. [CrossRef]
21. Dehghan, A.; Sedaee Sola, B.; Naderifar, A.; Gholampour, E. An Investigation on the Effects of the Reservoir Variables and Operational Parameters on Steam-Propane Injection Performance. *Pet. Sci. Technol.* **2013**, *31*, 1778–1789. [CrossRef]
22. Al-Murayri, M.T.; Maini, B.B.; Harding, T.G.; Oskouei, J. Multicomponent Solvent Co-Injection with Steam in Heavy and Extra-Heavy Oil Reservoirs. *Energy Fuels* **2016**, *30*, 2604–2616. [CrossRef]
23. Zare, A.; Abdulhameed, F.M.; Hesland, B.; Hamouda, A.A. Enhanced Heavy Oil Recovery (SAGD), Coinjection of Steam and Solvent, Reduction of CEOR and CSOR. *Pet. Sci. Technol.* **2017**, *35*, 570–577. [CrossRef]
24. Al-Muntaser, A.A.; Varfolomeev, M.A.; Suwaid, M.A.; Saleh, M.M.; Djimasbe, R.; Yuan, C.; Zairov, R.R.; Ancheyta, J. Effect of Decalin as Hydrogen-Donor for in-Situ Upgrading of Heavy Crude Oil in Presence of Nickel-Based Catalyst. *Fuel* **2021**, *313*, 122652. [CrossRef]
25. Sheng, K.; Okuno, R.; Wang, M. Dimethyl Ether as an Additive to Steam for Improved Steam-Assisted Gravity Drainage. *SPE J.* **2018**, *23*, 1201–1222. [CrossRef]
26. Nasr, T.N.; Kimber, K.D.; Vendrinsky, D.A.; Jha, K.N. Process Enhancement in Horizontal Wells through the Use of Vertical Drainage Channels and Hydrocarbon Additives. In Proceedings of the SPE Western Regional Meeting, OnePetro, Long Beach, CA, USA, 20–22 March 1991.
27. Keshavarz, M.; Okuno, R.; Babadagli, T. Optimal Application Conditions for Steam/Solvent Coinjection. *SPE Reserv. Eval. Eng.* **2015**, *18*, 20–38. [CrossRef]
28. Al-Muntaser, A.A.; Varfolomeev, M.A.; Suwaid, M.A.; Yuan, C.; Chemodanov, A.E.; Feoktistov, D.A.; Rakhmatullin, I.Z.; Abbas, M.; Domínguez-Álvarez, E.; Akhmadiyarov, A.A.; et al. Hydrothermal Upgrading of Heavy Oil in the Presence of Water at Sub-Critical, near-Critical and Supercritical Conditions. *J. Pet. Sci. Eng.* **2020**, *184*, 106592. [CrossRef]
29. Chemodanov, A.E.; Akhmadullin, R.R.; Sudakov, V.A.; Usmanov, S.A.; Khayrtdinov, R.K. Geochemical Modeling with the Use of Vertical and Horizontal Relative Concentrations of Oil Compounds for the Heavy Oil Fields. *Pet. Sci. Technol.* **2018**, *36*, 1100–1106. [CrossRef]
30. Minkhanov, I.F.; Bolotov, A.V.; Al-Muntaser, A.A.; Mukhamatdinov, I.I.; Vakhin, A.V.; Varfolomeev, M.A.; Slavkina, O.V.; Shchekoldin, K.A.; Darishchev, V.I. Experimental Study on the Improving the Efficiency of Oil Displacement by Co-Using of the Steam-Solvent Catalyst (Russian). *Oil Ind. J.* **2021**, *2021*, 54–57.

31. Varfolomeev, M.A.; Yuan, C.; Bolotov, A.V.; Minkhanov, I.F.; Mehrabi-Kalajahi, S.; Saifullin, E.R.; Marvanov, M.M.; Baygildin, E.R.; Sabiryanov, R.M.; Rojas, A. Effect of Copper Stearate as Catalysts on the Performance of In-Situ Combustion Process for Heavy Oil Recovery and Upgrading. *J. Pet. Sci. Eng.* **2021**, *207*, 109125. [CrossRef]
32. Minkhanov, I.F.; Marvanov, M.M.; Bolotov, A.V.; Varfolomeev, M.A.; Khairtdinov, R.K. Improvement of Heavy Oil Displacement Efficiency by Using Aromatic Hydrocarbon Solvent. *Int. Multidiscip. Sci. GeoConf. SGEM* **2020**, *20*, 711–718.